

On the quality of broadcast services in vehicular ad hoc networks

Dario Rossi¹ Roberta Fracchia², Michela Meo³,

¹TELECOM ParisTech, INFRES Department, Paris, France

²THALES, Land & Joint Systems Communications, Paris, France

³Politecnico di Torino, DELEN Department, Torino, Italy

Summary

We investigate the broadcast problem in suburban and highway inter-vehicular networks, aiming at providing a definitive comparison of two antipodean broadcast algorithm classes: the first one makes use of some *instantaneous information* locally available at the vehicles (such as vehicle position and speed), while the second one relies on *long-term knowledge* gained through a beaconing procedure. Using a realistic microscopic model to represent the vehicular traffic flow, we investigate the performance of the above broadcast algorithm classes by simulation, considering different classes of network services (e.g., Critical, Normal and Low-priority). In order to explore a very large algorithmic design space, we devise a Convex Hull framework that allows us to effectively compare and compactly present the boundaries of the solution space for each algorithm class. By the use of such framework we show that the beaconless performance encompasses a wider spectrum with respect to the beaconsed one, with lower complexity and overhead.

Copyright © 0000 John Wiley & Sons, Ltd.

KEY WORDS: Broadcast; QoS; VANET

1. Introduction

The last years witnessed an evergrowing thirst for connectivity, which is pushing for the deployment of communication devices along new roads – precisely those where the nodes of vehicular networks (VANETs) are traveling along. As entertainment applications may still favor unicast communication, infrastructured networks may be necessary to cope with such demanding requirements. At the same time, many useful services can still be successfully built on top of purely ad hoc multi-hop broadcast communication: that is, all kind of information

exchange that is relevant only within precise geographical boundaries and that targets unknown receivers. For instance, this will be the case for geo-contextualized advertisement (e.g., tourist and sight-seeing information, restaurants and hotels in vicinity advertising low rates to fill their vacancies), traffic related information (e.g., concerning traffic intensity and road-works, integrating and complementing the GPS-based navigation systems) or warning systems (which are paradoxically brought as example of “killer application” in VANETs). Notice that the source of information can be either initiated by vehicles (as in case of warning messages due to accidents) or by road-side units (as in the case of geographical advertisement and road-works) and then relayed in

*Correspondence to: D.Rossi, TELECOM ParisTech, France, E-mail: dario.rossi@enst.fr

Copyright © 0000 John Wiley & Sons, Ltd.

Prepared using *secauth.cls* [Version: 2008/03/18 v1.00]

ad hoc fashion by VANET nodes. Notice also that the above services have rather different QoS requirements: safety systems need a timely message propagation and a reliable coverage of the VANET. Conversely, geo-contextualized advertisement is subject to less stringent constraints, and it may be more interesting to charge content advertisers at different rates depending on the offered coverage.

Irrespectively of their QoS constraints, all the above services have nevertheless a common point: that is, as messages are relevant only in a given geographical area, they should cease to be relayed outside the road stretch they pertain to. We may thus define this communication paradigm as a “spatially-constrained” broadcast: given the appropriate context, we coin the *roadcast* neologism and use both terms interchangeably in the following. Roadcast communication may exploit two antipodean distributed paradigms: the *beaconless* approach relies on *instantaneous* information locally available at the vehicle, such as position and speed, whereas the *beaconed* one exploits a *long-term knowledge*, maintained through the exchange of beacons. This work extends [1], exploring the benefits of both the approaches in an exhaustive and systematic comparison: our aim is to find which paradigm is the most appropriate one to implement roadcast services, with different QoS requirements, in suburban and highway VANETs. We focus on a scenario in which all vehicles are equipped with GPS and, when communicating to each other, they piggyback their position in the exchanged packets. Using a realistic microscopic model to represent the vehicular traffic flow, we investigate and compare the performance of the above systems by simulation. For simplicity, we assume that service penetration is 100%, but other scenarios could be easily analyzed, leading to results that are equivalent to those reported here at lower densities. Indeed, the VANET is formed exclusively by those vehicles that adopts the considered technology and subscribe to the provided services. Information is then diffused over the VANET as long as nodes are connected with each other and their density is large enough to guarantee connectivity. If penetration is low, say only a fraction x of the vehicles are participating to the network, in a scenario with vehicle density γ the network results to be “equivalent” to a network with density $x\gamma$ and penetration 100%. While from the point of view of the network the two cases, 100% penetration and density $x\gamma$ or penetration x and density γ , are equivalent, the effectiveness of the service itself might be compromised under

low penetration rate. For example, in case of safety applications, the fact that only a fraction of vehicles are informed of a dangerous situation ahead in the way reduces the effectiveness of the safety application itself; other applications, such as location-based information delivery are instead not that sensitive to penetration rate, as far as the network is connected and service delivery is feasible. In this paper we do not analyze the effect of penetration based on the kind of service, but, rather, we focus on the performance of the network.

As simulation results forcibly reflect several modeling simplifications, rather than precisely quantifying the performance of a specific approach, we prefer to define the *boundaries* of the solution space inside which realistic performance figures may lie. To this purpose, we devise a framework based on the Convex Hull concept to assist the design and evaluation of VANET roadcast algorithms. The Convex Hull representation allows us to explore a rather large number of both *design* (e.g., roadcast algorithm class and settings) and *environmental* factors (e.g., vehicular traffic models and vehicle density, wireless channel). In this work, we investigate several *thousands* parameter combinations, and express the QoS of the roadcast service using the following performance indices: *reliability*, defined as broadcast message reception probability in the relevant road stretch; *redundancy*, the number of relay nodes involved in the propagation of a broadcast message; and *timeliness*, the reception delay at the end of the relevant road stretch. As different applications need different levels of QoS, the analysis will be carried on considering different classes of service (namely, Critical, Normal and Low-priority traffic), investigating their performance in details.

This work makes the three following contributions. First, we introduce a framework to assist the design and evaluation of roadcast communication algorithms: indeed, Convex Hull not only allows a compact representation of a huge parameters space, but is also helpful in its investigation, as it permits to build automated procedures to assist the parameter tuning task. Second, by applying the above framework, we are able to explore a rather large design parameter space by simulation: interestingly, we find that beaconless performance is a superset of beaconed performance. In other words, the performance boundaries of the beaconless procedure are wider than that of beaconed algorithms: this suggest that, through careful parameter selection it is possible to find beaconless algorithms that, at least

for the considered scenarios performs better than the broadcast ones. Third, we find that, in the beaconless case, vehicles may reduce the impact of flooding by simply taking into account their own speed: e.g., nodes deduce from their low speed that there is some congestion and, thus, reduce the probability of relaying the received information. To the best of our knowledge, this is an original result which has not yet been pointed out by other researchers. As a result, beaconless may be more suited than beaconed to handle suburban and highway VANETs scenarios, with limited broadcast traffic. On the one hand, at low densities (i.e., when the network is thus in danger of disconnection), the very same redundancy of beaconless approaches is the necessary condition for an increased reliability. On the other hand, provided the beaconing overhead is considered as well, the beaconless redundancy does not necessarily introduce a significant overhead compared to beaconing: rather, in some circumstances the *overall* number of messages transmitted under the beaconless paradigm is actually lower than the one of beaconed.

The remainder of this paper is organized as follows. Sec. 2 places our work in the context of related effort. After formalizing the beaconless and beaconed classes in Sec. 3, we describe in Sec. 4 the assumptions of the system under analysis. Then, after introducing the Convex-Hull framework in Sec. 5, we report simulation results on QoS evaluation of the roadcast service in Sec. 7. Finally, Sec. 8 concludes the paper.

2. Related Work

The broadcast problem has been extensively studied in the MANET context, whose results have been the natural starting point for VANET research as well: therefore, this research field is only relatively new. At the same time, as firstly pointed out in [2], due to the intrinsic differences of these networks the most promising routing strategies are not as effective as for the MANET context when they are applied to VANETs.

As a result, research work such as [2,3,4,5,6,7,8,9] focused on issues tied to realistic mobility models for VANETs. Authors in [3] propose vehicular traffic models, alternative to Random Waypoint commonly used in ad hoc research, that are based on real street map and traffic informations. An integrated mobility and traffic model is the focus of [4], whereas [5] proposes and validates a methodology to extrapolate mobility model from real user traces. Work such

as [7, 8, 9] focus instead on the impact of mobility model on the ad hoc network properties and protocol performance. The impact on network connectivity of different microscopic models of vehicular highway traffic is explored in [6, 7], while [8] studies mobility model impact on routing algorithms and [9] focuses on the topology of the ad hoc network in urban environments. All the above work agree that the underlying mobility model is a delicate issue, as properties and performance may change radically over different models. As such, researchers are aware that, though VANET inherit much from research on ad hoc and MANETs, algorithms cannot be imported “as is”.

Therefore, much valuable effort have been devoted to investigating multiple perspectives of vehicular networks [10, 11, 12, 13, 14, 15, 16, 17, 18, 19, 20, 21, 22, 23, 24, 25]. Data diffusion in VANETs have been investigated at different layers of the networking stack (e.g., MAC [10] or routing [11, 12]), in different environment (e.g., urban [13, 14] or highway [15]) possibly exploiting power control to shape the vehicular topology [16, 17]. Moreover, other research efforts [18, 19] have been fueled by the definition of an amendment to the IEEE 802.11 standard, namely 802.11p [26], also known as Wireless Access in Vehicular Environments (WAVE). Rather typically, the data diffusion application is a warning system for rapid broadcast propagation of safety-related information [20, 21, 22, 23, 24, 25]. In more detail, [20, 21, 22, 23, 25] focus on protocols for congestion control for emergency warning system, while [24] prototype and implement a Message Dispatcher, which is an interface between multiple safety applications and the lower-layer communication stack. Usually, such schemes adopt CSMA at the MAC layer, unlike [25] which proposes and evaluate a TDMA protocol.

Usually however, systems performance are proposed and evaluated *in isolation*: indeed, fewer work exists [27, 28, 29, 30, 31] that attempt to provide a *comparison* of different approach in the VANETs, in either a qualitative [27, 28] or quantitative [29, 30, 31] way. In more details, [27] qualitatively compares different MAC schemes, namely AD-HOC [32] and 802.11p to be used in VANETs, whereas [28] present a comprehensive qualitative comparison of unicast routing schemes in VANETs. Unicast routing schemes are instead quantitatively compared by authors in [29] which considers namely AODV [33] and GPSR [34], but also in [30] which contrasts AODV [33] to DSR [35], and in [31] which compares DREAM [36] and SIFT [37].

This work shares the same comparison spirit of [29, 30, 31], but focuses on multi-hop *broadcast communication*, rather than on unicast routing. Under this light, the work closest to ours are [38, 39], which compare beacon-less strategies versus beacon-based approaches in the MANET context. Yet, we point out that [38, 39] adopt rather simple mobility models that neglect the existence of correlation among the mobile nodes which is known to play an important role in determining the achievable performance [3, 4, 5, 7, 8, 9]. As such, beacon-less strategies versus beacon-based strategies have not been systematically explored in the VANET context. We stress that the aim of this work is not to propose yet another broadcast algorithm specifically designed for VANETs. Rather, our aim is to consider the research already performed as a starting point for the comparison. Indeed, we point out that during the last few years, several *beaconed* [34, 36, 40, 41, 62] and *beaconless* [20, 22, 39, 42, 43, 44, 45, 46, 47, 48, 49] algorithms have been proposed and analyzed in the VANET context. In the following, we briefly overview these algorithms, that we use as guidelines to define a general framework apt at describing the whole beaconed and beaconless algorithm classes.

Generally speaking, the beaconing [34, 36, 40, 41] information is used either in a *position* based fashion or a *topology* based fashion, although the latter approach is not suitable for VANETs as pointed out in [40]. Position-based routing can be mainly divided in *geographic forwarding* [34], where each node forwards incoming packets to exactly *one* of its neighbors, and *restricted flooding* [36, 41, 62], where flooding is restricted to a certain region of the network: the *beaconed* algorithms considered in this work belong to the latter family.

Beaconless algorithms are instead the object of [20, 22, 39, 42, 43, 44, 45, 46, 47, 48, 49]. The larger number of existing studies also reflect a greater freedom in the design space with respect to the beaconed case. Yet, all the above algorithms all have strong similarities and common points in the rebroadcast decision process. More precisely, the idea of letting the decision process depend on the distance is already present in [42], although the decision process is threshold-based rather than probabilistic. A uniform distributed waiting time is present in [39], whereas in [22, 43, 44, 48] the waiting time depends on the position of the previous transmitter and on the destination node. Additionally, in [22] the vehicular density is taken into account in the delay function. Finally, [49] considers the information propagation dynamics under the light

of the publish/subscribe paradigm, where the aim is to keep the information available during a given lapse of time: in this case, the aim of the decision process is to determine the number of relays which has to hold replicas of the messages that are then disseminated periodically, i.e., in multiple broadcast cycles, to the interested subscribers. We tackled the study of multiple broadcast cycles with an analytical approach in [50]; in this work, we will rather focus on the performance of different class of algorithm, during a single broadcast cycle, considering that all vehicles are interested with respect to the perspective adopted in [49].

We point out that it is difficult to provide a *direct* comparison of the above beaconed [34, 36, 40, 41, 62] and beaconless [20, 22, 39, 42, 43, 44, 45, 46, 47, 48] approaches, in reason of the different assumptions, scenarios and parameters used in the evaluation. Our work attempts at encompassing the above research, by providing a common framework where all the above algorithms fit – which we believe to be a first, necessary step for their comparison.

3. Roadcast Algorithm Classes

To compare the beaconed and beaconless paradigms, we have to define representative examples of both broadcast classes. For reference purpose, we provide the overall taxonomy of the considered classes in Fig. 1. Both beaconless and beaconed algorithms are constituted by two phases: during the *inference* phase, information about the VANET neighborhood is gathered, which is later used during the rebroadcast *decision* phase. In our framework, different *functions* are used to represent different algorithms within each class, whose behavior is further dependent on both physical and free *parameters*, as well as on the *variables* measured by vehicles prior (beaconed) or during (beaconless) the roadcast procedure. We report further details on the functions, on the variables they depend on, and on the parameter they use in the following sections and on Tab. I and Tab. II. However, prior to give further details on the formal framework definition, let us anticipate the general idea of the beaconless and beaconed classes, as well as illustrate their expected behavior and characteristics.

Beaconed approaches [34, 36, 40, 41] exploit a distributed mechanism, called beaconing, to proactively and periodically exchange information to keep a complete view of their neighborhood. The amount and quality of the information depend on

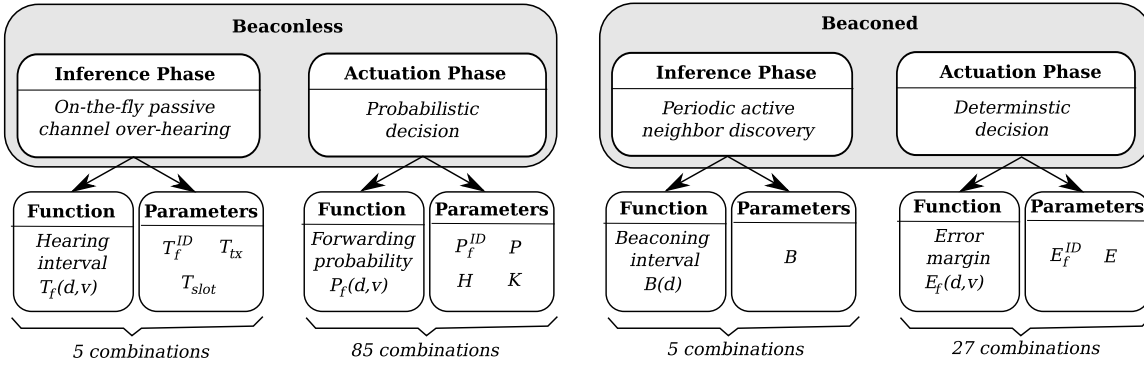


Fig. 1. Taxonomy of broadcast services: specific algorithms are determined by the choice of a *functional* relationship with the measured variables, and the settings some *parameters*. The table also report the number of combinations of function and parameters explored, that will be listed later on in Tab. I and Tab. II.

the frequency of the beacon exchange and, provided that information is refreshed at a high pace, nodes also have an up-to-date view of their neighborhood. As such, they can *deterministically* decide if their rebroadcast is *necessary* to extend the coverage. In this case, it is possible to introduce mechanism, such as error margins, to cope with *inaccurate* information (e.g., due to shaky or out-of-date GPS position). In a sense, by design, beaconsed solutions strive to minimize the number of relay nodes, converging to connectivity performance.

Beaconsless approaches [20, 22, 39, 42, 43, 44, 45, 46, 47, 48] resort instead to *passive channel overhearing* for the neighborhood discovery. This inference phase may only greedily exploit instantaneous information, is started on the fly and lasts a random waiting time. As such, vehicles knowledge of the neighborhood will be much more imprecise allowing to gather only a partial view of the neighborhood. After this phase, a *probabilistic rebroadcast* decision is taken to cope with such *incomplete* neighborhood information. Therefore, by design, we may say that beaconsless algorithms *introduce redundancy* to compensate for this inaccuracy.

To more formally and systematically explore this tradeoff, we first need to individuate the specific *information* (i.e., variables) at our disposal under either paradigm, and further devise the general means for exploiting such information: in other words, the algorithmic *knobs* (i.e., functions) that can be tuned on the basis of the gathered information.

3.1. Beaconsless Paradigm

In all beaconsless algorithms, only those pieces of information that are locally available at the receiving node and at the transmitting node (by piggybacking information in the roadcast message) can be used. Here is a list of the instantaneous information that can be used by a beaconsless algorithm:

- **Transmission Range**, R , possibly piggybacked in the packet, or inferred by coupling the received signal strength and quality to the transmitter distance D information, or set according to the standard specification given for the adopted technology.
- **Distance from the transmitter**, D , possibly normalized over the transmission range, $d = D/R$. The distance is computed at the receiver through the instantaneous GPS position of transmitter, piggybacked in the message header, and the GPS position of the receiver. The distance d can be used to evaluate the additional coverage that the receiving node would achieve by retransmitting the message: the rationale is that the larger the additional coverage is, the higher the forwarding probability is.
- **Receiver speed**, V , possibly normalized over a maximum vehicular speed, $v = V/V_{\max}$. The speed can be used as an indicator of the local traffic conditions: in particular, small values of speed denote congested traffic (a jam, a platoon of vehicles close to each other and slaken by a slow vehicle, etc.). Under congested conditions,

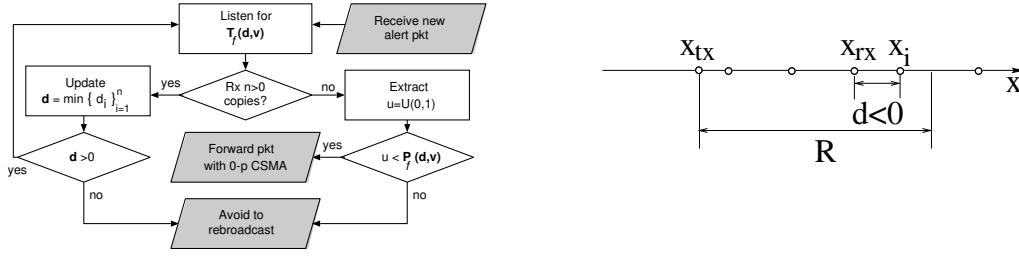


Fig. 2. Beaconless class: algorithms flowchart (left) and diagram illustrating used notation (right)

the network is connected and the forwarding probability can be set to small values to reduce the possibility of a broadcast storm.

- **Transmitter speed**, V_T , piggybacked in the roadcast message, normalized as $v_T = V_T/V_{max}$. We argue that v_T is not likely to be relevant and therefore we disregard it in the following: indeed, as the broadcast propagation occurs in the *opposite* direction with respect to the vehicles movements, the speed of the transmitter barely provides any useful information to the vehicles that follow.

Then, different knobs can exploit the above information, yielding to very different reliability and redundancy performance:

- **Delay of the first transmission attempt**, T_f , is the time after which the packet is handed to the MAC layer. The purpose is to create a short time window that allows the receiver to collect from the neighboring nodes a number of copies of the *same* roadcast message: the number of copies, combined with the information carried by the message, gives the receiving node some knowledge about its neighborhood (such as position and speed v_T). The larger T_f is, the more accurate the knowledge about the neighborhood is, but, also, the less timely the message propagation is.
- **Forwarding probability**, P_f , is the probability that the roadcast message is retransmitted. As already mentioned, the setting of P_f is the core of a beaconless algorithm, and trades off between the opposite needs of having high reliability and low redundancy.
- **Transmission power**, P_T . By properly setting P_T , a desired transmission range R can be selected. In general, this parameter is strongly dependent on the employed technology and

regulations cannot be easily changed, therefore we do not consider P_T as a free variable.

Several algorithms have been devised by differently combining the above information and knobs [20, 22, 39, 42, 43, 44, 45, 46, 47, 48]. We abstract the general idea of these beaconless algorithms in the left part of Fig. 2, reporting in the right portion of Fig. 2 a scheme useful to understand the notation we use. As soon as a node x_{rx} has received the first roadcast message from a node x_{tx} , it starts sensing the channel for a time T_f during which the node checks if other copies of the same message are received. Whenever n copies of the message are received during this waiting phase, the receiver evaluates the minimum distance from the transmitters x_i , $d = \min\{d_i\}_{i=1}^n$, with $d_i = x_{rx} - x_i$. If at last one node is further away along the road, i.e. $d < 0$, the receiver x_{rx} can safely avoid to forward the message: indeed, the message has already covered an area which is outside its transmission range and a re-broadcast would be useless. Otherwise, it suspends the decision and enters a new waiting phase T_f . In case no copies are received during T_f , the receiver x_{rx} forwards the message with a probability P_f .

Both T_f and P_f , the knobs of the beaconless algorithm, can be based on the information gathered during all the previous waiting phases: among the different available information we select the speed v and the minimum transmitter distance d observed during the waiting phase. Notice that the duration of the first waiting phase is determined by the distance between a single transmitter and the receiver, during which messages coming from further away relay nodes can be overheard (and d_{min} can be evaluated over several nodes). As a side note, we point out that, to the best of our knowledge, the idea of adapting the rebroadcast probability to the vehicular speed (which we will show to account for significant performance gain in Sec. 7) has not been used in the *beaconless* context so far (but only in the beacons approach [36]

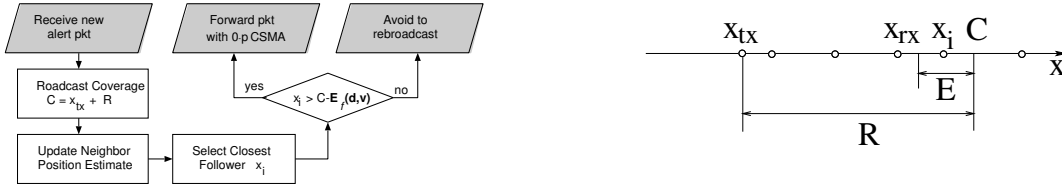


Fig. 3. Beaconed class: algorithms flowchart (left) and diagram illustrating used notation (right)

that adapts the rate of the beaconing procedure to vehicle speed).

In order to build a fairly large and representative subset of the beaconless class, we select a number of functions, indicated by different IDs in Tab. I, for setting the forwarding delay $T_f(d, v)$ and the forwarding probability $P_f(d, v)$. These functions, that make use of the transmitter distance d and receiver speed v , also depend on the packet transmission duration T_{tx} , the MAC time slot duration T_{slot} and on two free parameters, namely H and K . By abuse of notation, we indicate the functions by their corresponding ID, e.g., P_f^{ID} with $ID = 1$ indicates $P_f(d, v) = 1 - (1 - d)^K$ as in [48]. Notice that the forwarding probability $P_f(d, v)$ is also tuned according to the free parameters H and K , whose actual semantic is tied to the specific function P_f^{ID} reported in Tab. I.

A specific algorithm of the considered beaconless class can then be uniquely individuated by the tuple $(T_f^{ID}, P_f^{ID}, K, H) \in \mathbb{N}^4$. In what follows, we inspect the full cross product of functions $T_f^{ID}, P_f^{ID} \in \{0, 1, 2, 3, 4, 5\}$ and parameters $H, K \in \{1, 2, 4, 8\}$, as indicated in Tab. I, for a total of $6 \times 6 \times 4 \times 4 = 576$ different beaconless settings.

3.2. Beaconed Paradigm

Besides the information available in the beaconless case, a beaconing service may provide nodes with a more complete knowledge of the neighborhood within a one- or two-hops radius. However, two-hops information is mainly useful in MANETs (where nodes move at relatively slow speed in a bidimensional space), whereas a two-hop knowledge is redundant in case of homogeneous transmission range and outdated at much higher rate in VANETs (due to linear network topology and high speeds). Given this premise, we focus on algorithms that rely on:

- **Transmission Range, R .**

- **Distance from the transmitter, d .**
- **Receiver Speed, v .**
- **Estimated Neighbors Position**, obtained from the *position* and *speed* of one-hop neighbors, exchanged through a beaconing procedure.

In the beaconed case, the error of the transmitter and receiver position estimate can be used to correct other estimates. However, since a preliminary exploration has shown that the impact on performance of such correction mechanisms is marginal, we disregard them in the following.

Two general distributed approaches can be envisioned at this point, namely *receiver-based* or *transmitter-based* decision: in reason of its robustness in case of packet loss, in the following we focus on the former. As depicted in Fig. 3, upon reception of a message, the receiver vehicle x_{rx} updates the *estimate* of its neighbors' positions. Through the knowledge of the transmission range R , it estimates also the total distance C covered by the message, and the decision boils down to assessing whether the rebroadcast is *necessary* in order to extend the message coverage: x_{rx} identifies the closest following vehicle x_i and decides to rebroadcast the warning message only when this vehicle is beyond in the transmission range of the broadcast message sent by x_{tx} .

Notice that, as opposite to [62], which consider heterogeneous transmission ranges, we make the simplifying assumption that transmission range R is known and constant for all vehicles. Still, as the decision may be affected by several other estimation errors, we argue for the necessity of an error correction margin E in the decision process. Assuming to precisely know the transmission range, the error margin reduces the number of missed forwarding errors due to underestimation of neighbor's distance. In other words, to avoid network connectivity disruption, each vehicle rebroadcasts the message when the closest following vehicle is outside the coverage range (i.e., $x_i > C$) or inside the coverage range but within a distance E from the coverage

Table II. Vehicular, Networking and Environmental Parameters

| | |
|-------------------|--|
| Environment | Linear road stretch 10Km Relevant area L=2Km Beacon size SB = {20,500} Bytes |
| MAC Layer | Message size SM = {500,1000} Bytes Medium Access Control: 0-p CSMA Contention window CW = 31 slots Tslot = 20 μ s Transmission Range R = 200 m Data Rate C = 2 Mbps |
| QoS Metrics | Reliability: reception probability P Delay: delay D at distance L Redundancy: number of relay M |
| Roadcast Services | Critical: high reliability, low delay Normal: moderate reliability Low-priority: low cost, low overhead |
| Vehicular Traffic | ρ ID 2 {Gipps, Vdr, Toca, NaSch} $\rho = \{5i\}, i = 2..8$ $\rho_c = \{12..18\}$ CA and CM steps= 1.2 s CA cell = 7.5m |
| Wireless Channel | α ID = {Ideal, Bern, Trans} α Bern = {i/20}, i = 0..5 α Trans = {i/10}, i = 0..5 |

border (i.e., $x_i > C - E$), as depicted in the righthand side of Fig. 3. The error margin E can either be constant ($E_f(d, v) = E$ for $E_f^{ID} = 0$), or change as a function of the distance from the transmitter and of the vehicle own speed (for $E_f^{ID} > 0$).

As reported in Tab. I, in the beacons case we explore three knobs (B, E, E_f^{ID}), namely the beaconing interval B , the error correction margin E and the margin adaptation to the traffic condition through the E_f^{ID} function. Unless otherwise stated, the beacon packet size is 20 Bytes: later on we will explore the impact of larger beacon size (e.g., needed due to authentication or encryption for security purposes) on the system performance as well. The transmission frequency of beacon messages also impacts the performance of the beacons algorithm. We assume that beacons are exchanged periodically every B seconds: to avoid synchronization and reduce beacon collisions, the transmission of each beacon can be jittered as in [34], so that the inter-beacon transmission time is uniformly distributed in the interval $[0.5B, 1.5B]$.

The explored beacons design set (B, E, E_f^{ID}) is the full cross product of the sets $B \times E \times E_f^{ID}$, for a total of $5 \times 9 \times 3 = 145$ different settings.

4. System Assumptions

We evaluate roadcast performance using a custom discrete event simulator, that accurately describes both network and vehicular dynamics. The simulator is written in ANSI C and is available as open source software at [51]. In this section we detail the simulation scenarios, reporting for the sake of clarity all the described parameters in Tab. II.

4.1. Roadcast Scenario

We evaluate the effectiveness of roadcast services considering a VANET formed along a linear stretch of a suburban road or highway. The assumption of the road linearity bears additional discussion. First, being vehicles equipped with GPS, they are also likely equipped with a navigation system as well, meaning that a digital map is available at the receiver: in this case, the position advertised by transmitters in the broadcast packet can be re-mapped to a “linearized” road portion, and thus the actual road-distance (rather than the air-distance) could be easily considered. Moreover, road windings can be expected to occupy a relatively small highway portion compared to the roughly straight one. Finally, we believe the study of a linear road stretch to be a preliminary but necessary step, before more realistic but complex scenarios (e.g., involving intersections, highway overpasses and highway junctions) could be taken into account.

On such road, of which we simulate a 10 Km-long stretch, roadcast propagation may start from any traveling vehicle or stationary road-side unit, and is targeted to all vehicles within a *relevant area*, of length $L = 2$ Km: vehicles outside this area, instead, never relay the message, so that the medium remains available for other services. The message propagates in the opposite direction with respect to the vehicles movement and, hopefully, it should reach all nodes up to the last one in the roadcast area. In order to gather *conservative* results, we adopt a single-lane, single-direction scenario: several parallel lanes indeed increase the network connectivity [6], and a similar effect is induced when vehicles traveling in the opposite direction relay the non-pertinent messages *on purpose* [45].

4.2. MAC Layer

The simulator implements a MAC layer accurately modeling collisions and retransmissions. We assume

Table I. Algorithmic Design Space: Beaconless and Beaconed explored settings

| ID | $T_f(d, v)$ | $P_f(d, v)$ | $E_f(d, v)$ | Beaconed Parameters |
|----|------------------------------------|--|-------------------|----------------------------|
| 0 | $2T_{tx} + U(0, 31)T_{slot}$ | $P(\text{const})$ | $E(\text{const})$ | $E_f^{ID} \in \{0, 1, 2\}$ |
| 1 | $T_{tx} + U(0, (1-d)T_x)$ | $1 - (1-d)^K$ | vE | $B \in [1..5]$ |
| 2 | $T_{tx} + U(0, (1-v)T_x)$ | $1 - (1-v)^H$ | dE | $E = 2^i, i = [0..8]$ |
| 3 | $T_{tx} + U(0, (1-v)(1-d)T_x)$ | $1 - (1-d)^K(1-v)^H$ | - | Beaconless Parameters |
| 4 | $T_{tx} + U(0, \min(1-v, 1-d)T_x)$ | $1 - (1-d)^{K(v)}$, with $K(v) = 1 + (K-1)(1-v)^H$ | - | $T_f^{ID} \in [0..5]$ |
| 5 | $T_{tx} + U(0, (2-v-d)T_x)$ | $1 - (1-v)^{H(v)}$, with $H(d) = 1 + (H-1)(1-d)^K$ | - | $P_f^{ID} \in [0..5]$ |
| | | | | $H = 2^i, i = [0..3]$ |
| | | | | $K = 2^i, i = [0..3]$ |

that nodes are equipped with carrier sense capabilities and adopt a 0-persistent Carrier Sense Multiple Access (CSMA) mechanism, similar to the IEEE 802.11 MAC scheme: in order to avoid collisions, the nodes sense whether the channel is busy before starting a transmission. In case the channel is busy, the message transmission is delayed for an amount of time slots uniformly distributed between zero and the contention window size, until the medium is sensed idle. In the CSMA, the contention window is set to 31 time-slots and the time-slot is $T_{slot} = 20 \mu\text{s}$ long. We assume moreover that on-board devices transmit such messages at a $C = 2 \text{ Mbps}$ rate (to gather conservative performance results and since broadcast messages should use a robust modulation), with transmission range $R = 200 \text{ m}$ equal for all vehicles.

Unless otherwise stated, the roadcast message size is $S_M = 1000 \text{ Bytes}$ and, in case a beaconing service is used, the beacon size is $S_B = 20 \text{ Bytes}$. In Sec. 7, we will also explore different combination of roadcast (i.e., 500 or 1000 Bytes) and of beacon (i.e., 20 or 500 Bytes) message size, in order to refine the evaluation of the system overhead. We assume that messages carry a random identifier chosen by the source, which is cached by every receiver for a small amount of time: in this way, every node forwards the same message at most once.

4.3. QoS Metrics and Roadcast Services

Different classes of service are offered directly on top of the MAC layer, which makes sense layer

since a broadcast communication paradigm is used. As previously stated, roadcast services may have different QoS needs, expressed by a Service Level Specification (SLS). SLS defines the expected (or guaranteed) performance of the service in terms of the following metrics, summarized in Tab. II:

- *reliability*, expressed in terms of the broadcast reception probability P in the relevant stretch;
- *redundancy*, expressed in terms of the number of relay nodes, or, equivalently, the number M of messages transmitted per roadcast message;
- *timeliness*, expressed in terms of the reception delay D at the end of the relevant road stretch.

Different applications may attach to the above metric a different level of importance. Thus, we explore the system performance by explicitly taking into account the following QoS classes of roadcast services:

- the *Critical* class, used by safety information systems that aim at maximizing reliability and minimizing the reception delay;
- the *Normal* class, whose reliability constraints are less tight with respect to mission critical applications, used by traffic and road-work information systems or advertisement;
- the *Low-priority* class, whose traffic has no reliability constraints but should be provided at lower cost, as for instance the case of low-cost geographical advertisement.

4.4. Wireless Channel

No physical layer is actually implemented in the simulator, which does however take into account varying conditions of the wireless channel by means of two probabilistic packet-level error models, indicated by α^{ID} in Tab. II. Both are high-level models that describe packet loss probability, and in both cases all vehicles have the same wireless channel. In the simplest model, the probability that a message is not correctly received is Bernoulli with probability α , independent on the transmitter-receiver distance. As reported in Tab. II, we consider a loss probability α ranging from 0 to 0.25 (in steps of 0.05):

$$P_{Bern}(d) = \begin{cases} \alpha & \text{if } d \leq R \\ 1 & \text{if } d > R \end{cases}$$

Conversely, in the second model, loss probability depends on the distance between transmitter and receiver: indeed, it is well known that the electromagnetic signal degrades with the distance, and empirical studies [52, 53] show that a *transitional* region exists. We denote by αR the amplitude of the transitional region and we assume that:

- below $(1 - \alpha)R$, communications are lossless and undisturbed,
- within $(1 - \alpha)R$ and R , the packet loss probability linearly increases, and
- above R , that is outside the transmission range, communication will certainly fail.

Summarizing, we have

$$P_{Trans} = \begin{cases} 0 & \text{if } d \leq (1 - \alpha)R \\ \frac{d - (1 - \alpha)R}{\alpha R} & \text{if } (1 - \alpha)R < d \leq R \\ 1 & \text{if } d > R \end{cases}$$

where it is easy to gather that, for the transitional channel, the average channel loss probability is equal to $\alpha R/2$. Simulations are performed with α varying from 0 to 0.5 (in steps of 0.1), so that the average loss probability spans over the same ranges for both channels.

The above models, despite their simplicity, allow a first grade inspection of the system behavior in presence of non-ideal wireless channels. Besides, an advantage of this level of abstraction is that such models are not tied to a peculiar physical modulation, a specific hardware platform, or a given environment, but are applicable to a more general extent. Moreover, wireless channel models such as Gilbert's [54], which introduce *time-correlation* in the wireless channel, are

not suited for our setup: indeed, since the message propagation occurs only once along a given channel, the effect of the time-correlation is likely to be negligible during a single roadcast propagation. On the contrary, we expect the effect of the *space-correlation* introduced by the transitional model to play a remarkable role. Finally, we point out that while channel models for VANET started to appear [55], they are tailored for physical layer simulation, and thus can not be applied as-is in the current work.

4.5. Vehicular Traffic

As macroscopical description of traffic flows is known to bring unrealistic results [7, 9], we model VANET movements at a *microscopic* level, abstracting real drivers behavior in a few mathematical rules. In microscopic modeling, each vehicle is individually resolved: a vector of state variables (x, v) describes the spatial location and the speed of the vehicle along a one-dimensional road. A model consists of a set of equations to update the state vector over time, depending on the states of other vehicles around. Two classes of models currently in use, namely Cellular Automata (CA) and Coupled Maps (CM), display properties similar to the real traffic dynamics at a microscopic level. CA models are discrete in both space and time (as reported in Tab. II, space is measured in cells and time in steps, so that speed is expressed in cells per step), whereas CM models are continuous in space but still discrete in time. Already introduced in the 1950s, these microscopic modeling techniques have been increasingly used in the last decade [56, 57, 58, 59], because of their good match with empirical traffic measurements [60, 61].

Our simulator implements four different traffic models indicated by ρ^{ID} in Tab. II, namely, NaSch [56], VDR [57], TOCA [58] and Gipps [59], and we explore a total of 16 traffic densities ρ per model. For the sake of illustration, we describe the simplest of the above models, namely NaSch [56], while we refer the reader to [7] or the respective publications for further details concerning the others. The rules used by the NaSch model are:

$$\left\{ \begin{array}{l} \textbf{Behavioral Rules} \\ v \leftarrow \min\{v + 1, v_{max}\} \\ v \leftarrow \min\{v, g\} \\ v \leftarrow \max\{v - 1, 0\} \text{ w.p. } P_d \\ \textbf{Motion-update} \\ x \leftarrow x + v \end{array} \right.$$

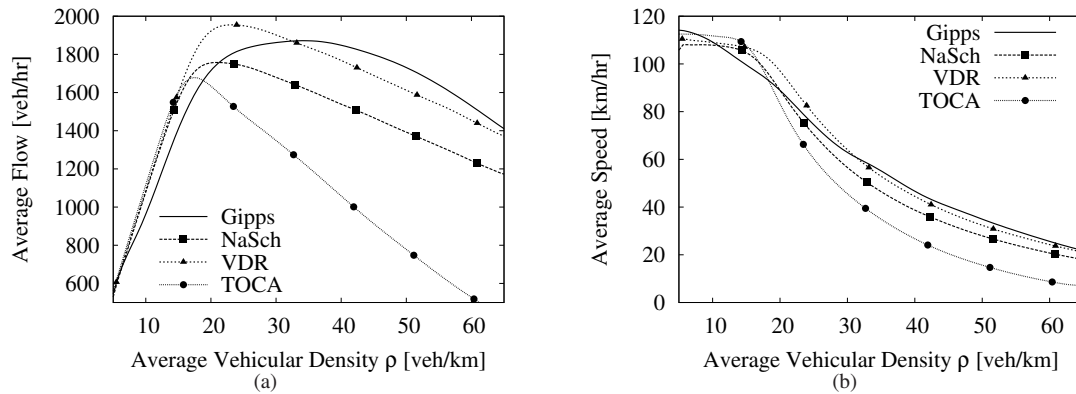


Fig. 4. Fundamental Diagram: (a) Average traffic flow and (b) Average speed at different vehicular densities.

The first two rules describe deterministic car-following behavior: drivers try to accelerate by one speed unit except when the maximum speed v_{max} is reached or when the gap g from the vehicle ahead is too small. The third rule introduces random noise: with probability P_d , a vehicle ends up being slower than what calculated deterministically; this parameter simultaneously models effects of (i) speed fluctuations at free driving, (ii) over-reactions at braking and car-following, and (iii) randomness during acceleration periods. Due to the parallel update, an implicit reaction time of the order of the timestep is introduced; however, rather than representing the actual driver's reaction time, which would be much shorter, the reaction time is a measure of the time elapsed between the stimulus and the action of the vehicle. Finally, vehicle positions are updated with the new speeds.

Such models reproduce the most important characteristics of the real traffic dynamics [60, 61]: that is, the phase transitions exhibited by the vehicular speed, due to the spatial correlation of vehicles. This behavior is clearly visible in Fig. 4, which contrasts the typical measurement of traffic flow of the CA and CM models early introduced, i.e., the so-called *fundamental diagram*. The fundamental diagram depicts the traffic flow (left hand-side plot) expressed in vehicles per hour, and the average vehicle speed (right hand-side plot) as a function of the density ρ in vehicles per kilometer. The typical transition happens whenever the average vehicular density ρ increases above a critical density ρ_c : the system passes from the *free-flow* regime (where vehicles move nearly at maximum speed without interference from other vehicles) to a *congested* state (where vehicular flow and density are strongly correlated and velocity

decreases). An important point to stress here is that, as the vehicle density is variable in both time and space, actually, there are periods and areas in which density of vehicles much higher than the average ρ can be observed: notably indeed, platoon of cars may form already in free-flow, whereas traffic jam happens whenever the *average* density exceeds a critical density.

Then, an interesting remark is that, although all models reproduce the typical shape of the fundamental diagram, some discrepancies arise: these are due to the different behavioral rules adopted to mimic drivers' reaction to the external traffic conditions. Also, the transition between states is evident in both the flow as well as the velocity curves of Fig. 4, though the actual slopes differ from model to model. In particular, the most significant differences appear in congested states where inter-model differences, due to the specific driver behavioral rules, are more pronounced. We point out that each model captures different aspects of the complex vehicular movement dynamics, and that no universally accepted model has emerged yet: therefore, considering several models is necessary to gather realistic performance boundaries.

5. Methodology

We assess the system performance by running an extensive set of simulations. To clarify our terminology, in the following we refer to simulation *point* as the result of several thousand simulation *runs*, whose stop criterion is that significant variables achieve a confidence level of 99% and a confidence

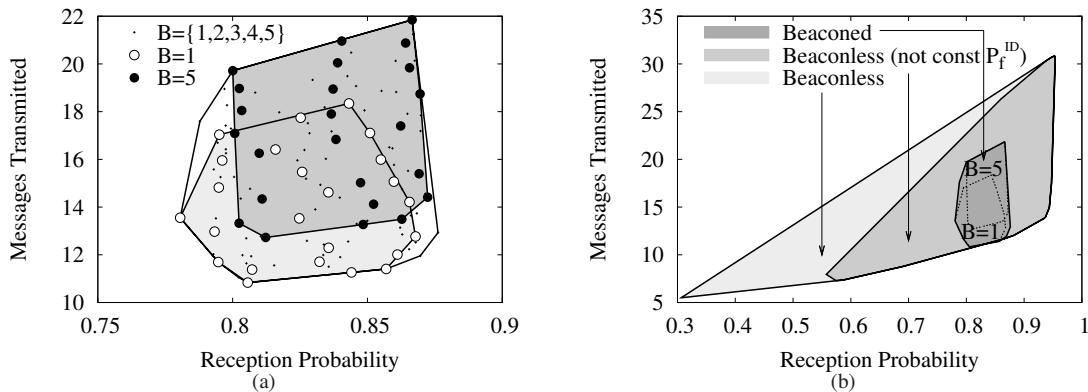


Fig. 5. Convex Hull: Beaconsed (a) and whole (b) design spaces for $\rho = \rho_c$ and a wireless error-free medium.

interval of 2%. Each simulation *point* corresponds to a full tuple of environment settings $(\rho^{ID}, \rho, \alpha^{ID}, \alpha)$ and algorithm settings for the beaconsed (B, E, E_f^{ID}) and beaconsless $(T_f^{ID}, P_f^{ID}, K, H)$ cases. Overall, the analysis of the full set of parameters reported early in Tab. II would yield to a total of $4 \times 14 \times 2 \times 6 = 672$ combinations of vehicular traffic and wireless errors per single algorithmic setting, which would lead to $672 \times (145 + 576)$ or nearly 500,000 different combinations to explore – a definitively too vast parameter space. Luckily, following [1] we can build a more efficient investigation path, as VANETs connectivity can be split into three different regions:

- *below* the critical threshold $\rho < \rho_c$, the reception performance is mainly driven by the network connectivity – thus, beaconsed or beaconsless paradigms only play a minor role in determining the performance;
- the region *around* the critical density $\rho \simeq \rho_c$ is also critical with respect to reliability – as this performance metric is heavily influenced by both the vehicular traffic model and the specific implementation of the roadcast service;
- *above* the threshold $\rho > \rho_c$, the VANET is connected and broadcast communication is very reliable irrespectively of the adopted paradigm – conversely, the number of exchanged messages differs significantly in this zone depending on the broadcast service class.

The above observations have some important consequences. First, the roadcast implementation mainly affects the reliability performance *around the*

critical vehicular density ρ_c : this region is therefore the most suited one to tune the algorithm setting aiming at *maximizing the packet reception probability* P . We point out that this region constitutes a stiffer scenario, where the reliability of Critical network services may be compromised. This corresponds to very hazardous situations, where a high number of vehicles moving at a relatively high speed may be forced to abruptly slow down, suddenly braking to avoid an accident. Consequently, as early reported in Tab. II, we employ a finer granularity around the critical threshold $\rho_c \simeq 15$. Second, as redundancy varies widely at *high vehicular traffic densities* $\rho > \rho_c$, this region is the most suited one to tune the algorithm setting aiming at *minimizing the number of transmitted messages* M . Our exploration of the algorithmic design space will follow the above guidelines, so to reduce the number of simulations to a more manageable amount. In our framework, we first tune first the most critical performance parameter (reliability), then we reduce the design space by tuning the remaining metric (redundancy). However, prior to report the simulation results, let us describe the convex hull framework that we will use in the following.

5.1. Convex Hull Representation

Without loss of generality, let us start by considering the reception probability P and the number of relay messages M : intuitively, these metrics tradeoff, as the redundancy M is the price to be payed in order to achieve a reliability level P . We can explore this tradeoff adopting a Convex Hull representation:

to put it simply, we plot the (P, M) couples in a bidimensional cartesian space, then find the smallest closed line that encloses all the points. This representation has several advantages: first, it is very compact, and therefore allows us to explore a very wide number of scenarios at once. Second, it is still possible to understand the impact of each parameter in isolation by partitioning the hull over that parameter (i.e., by conditioning the results). Finally, it is possible to build semi-automated processes that helps in tuning the design space.

For the sake of illustration, the convex hull of the whole beaconsed design space is depicted in Fig. 5-(a) for $\rho = \rho_c$ and a wireless error-free medium, which corresponds to 145 simulation points – each of which, we recall, is the result of several thousands simulation runs, and thus each (P, M) couple is statistically significant. We report also the individual simulation points corresponding to the beaconsed hull conditioned over $B = 5$ with filled circles, over $B = 1$ with empty circles and the remaining points with small dots. It can be seen that, irrespectively of the algorithmic function and parameters (i.e., E_f^{ID} , E and B) the beaconsed performance are very similar: indeed, the curves of the $B = 5$ and $B = 1$ cases almost overlap, and individual points are scattered within the whole hull. In other words, the hull spread is not related to design parameters, but rather to environmental factors – such as, in this case, the traffic model.

As a further example, we report in Fig. 5-(b) the whole beaconsed and beaconsed design spaces, again at $\rho = \rho_c$ and for a wireless error-free medium. The dataset represented in Fig. 5-(b) corresponds to about 720 simulation points, and we now report only the hulls, hiding the individual points. As far as the beaconsed algorithms are concerned, we report both the whole space and the same breakdown (i.e., $B = 1, B = 5$) reported above in Fig. 5-(a). In the beaconsed case, we report both the whole space and the hull which excludes algorithms using a constant rebroadcast probability. Notice that beaconsed results are much more clustered than the beaconsed performance that presents a wide dispersion. Beaconsed performance is a *superset* of beaconsed performance, in the sense that the beaconsed hull is entirely contained in the beaconsed hull. These results suggest that the beaconsed approach has a larger variability of possible performance with respect to the beaconsed approach and the algorithm can be tailored, based on the service to provide, to satisfy the desired trade-off between accuracy and overhead. Moreover, beaconsed can achieve better performance

than beaconsed (a higher reception probability is possible). However, the cons of this is that parameter setting is more critical in the beaconsed than in the beaconsed approach, so that a wrong setting might lead to significant worse performance.

5.2. Partitioning the Convex Hull

In order to trim the design space, we adopt, in parallel, two different tuning approaches. A first approach is to *filter* the solution space, in order to prune the settings that do not comply with a target SLS profile, specified by means of *absolute* thresholds. For instance, we may upper-bound the number of relay in Low-priority service $M(\rho > \rho_c) < M^*$, or lower-bound the reliability of Critical services $P(\rho \simeq \rho_c) > P^*$, or jointly constrain Normal services to $P(\rho \simeq \rho_c) > P^*$ and $M(\rho > \rho_c) < M^*$. The main advantages of the filtering approach is that, besides allowing to quickly reduce the design space, the remaining solutions are already compliant with the target SLS. In other words, filtering will isolate specific algorithmic settings, that is, (B, E, E_f^{ID}) tuples in the beaconsed case and $(T_f^{ID}, P_f^{ID}, K, H)$ tuples in the beaconsed one, that can be used to implement a given QoS service.

Yet, care is needed to avoid discarding potentially interesting solutions, due to an unfortunate choice of the thresholds: in order to avoid this problem, a *relative* performance comparison is desirable. This is the approach that we adopt in a *dicotomic* methodology, that we present with the help of Fig. 6. For instance, let us consider the design of a Normal service, where we want to achieve a good reliability P limiting at the same time the overhead M . Starting from the whole solution space of the beaconsed class, which includes all possible algorithmic parameters, we *split* the hull around the median reliability, gathering two semi-planes: i.e., in the upper-reliability U and low-reliability L semi-planes. We then split each reliability semi-plane around the median redundancy, obtaining the UU, UL and LU, LL quarter-planes. Intuitively, algorithms falling in the LL plane will provide poor reliability but low overhead; UL algorithms will provide better reliability at increased cost, and UU will provide highest reliability at the highest cost; LU are instead poor performing algorithms, providing low reliability at a furthermore high cost. The splitting process is then *iterated*: in case of Normal service class, a natural choice would be to select the high-reliability low-redundancy UL quarter-plane for the next iteration.

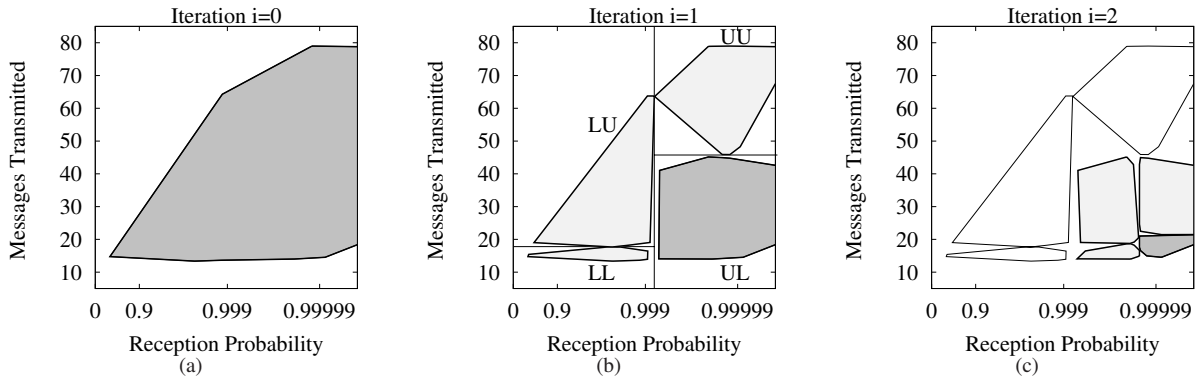


Fig. 6. Example of dicotomic iterative hull partitioning: initial hull (a), first (b) and subsequent iterations (c).

Iterations continue until either (i) selected solutions are compliant to the target SLS, or (ii) the solution set reaches a minimum cardinality threshold, or (iii) the maximum number of iteration is reached.

Fig. 6 illustrates the iterative UL splitting process. Fig. 6-(a) shows the initial hull, when no other filtering has been performed, for the beaconless algorithms class at high vehicular traffic densities on an error-free medium. As expected, reliability is very high, since already after the first iteration $i = 1$, reported in Fig. 6-(b), half of the beaconless settings (i.e., the UU and UL quarter planes) achieve $P > 0.999$. However, further iterations of dicotomic splitting can be used to find settings that reduce the number of broadcast messages: in this case, applying a second splitting iteration $i = 2$ to the dark-gray UL hull of Fig. 6-(b), is sufficient to find specific settings that significantly limit the number of messages that have to be broadcasted, as it can be seen from the dark-gray UL hull of Fig. 6-(c).

Then, depending on the specific stop condition, iteration may continue, which is not shown in Fig. 6 to avoid cluttering the pictures. Thus, splitting the hull equals to select specific algorithmic settings, whose performance comply to a given SLS. More precisely, we define the following dicotomic hull partitioning strategies, that are tailored for the different class of services under consideration:

- Critical service: UL splitting at first iteration, UU splitting at subsequent iterations;
- Normal service: UL splitting at all iterations;
- Low-priority service: UL splitting at first iterations, LL splitting at subsequent iterations.

6. Simulation Results

In this section, we explore the design space of beaconless and beacons classes described in Sec. 3, investigating their sensitivity to the environmental and scenario parameters reported in Sec. 4. As noted Fig. 5-(b), beacons performance are more compact: basically, beacons provides a unique service class \mathcal{B} , which offers a reliable and effective roadcast transmission. Conversely, beaconless performance are much more spread out, and the tuning of several parameters is key to offer different classes of service. In the beaconless case, we thus consider different set of parameters, that correspond to the different service classes early introduced:

- Critical set (\mathcal{C}), gathered by filtering;
- Normal set, gathered by either filtering (\mathcal{N}_f) or dicotomic partitioning (\mathcal{N}_d);
- Low priority set (\mathcal{L}), gathered by dicotomic partitioning.

6.1. Ideal wireless channel

Let us start by considering in Fig. 7-(a) the performance of the different services around the critical density ρ_c for an error-free wireless medium. Several hulls are reported in the picture, such as the \mathcal{B} hull, corresponding to the whole design space of the beacons approach, and a few beaconless groups, tailored for the different QoS levels described above. In case of beacons algorithms, performance is much more clustered and individual points are scattered within the whole hull, so that environmental

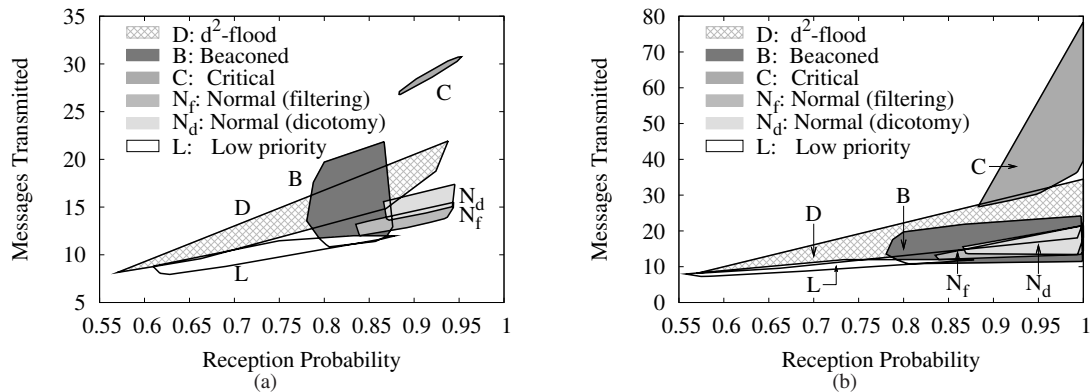


Fig. 7. Beaconed (\mathcal{B}) and beaconless ($\mathcal{C}, \mathcal{D}, \mathcal{N}_f, \mathcal{N}_d, \mathcal{L}$) performance (a) at density ρ_c and (b) at jammed vehicular densities

parameters drive performance more than algorithmic settings. Intuitively, this is a result of the beaconed design, which tries to build a precise view of the VANET topology, aiming at jointly maximizing the roadcast reliability and minimizing the number of transmissions for the roadcast service.

Beaconless performance are instead more dispersed. Fig. 7-(a) reports for reference the hull corresponding to $(0, 1, K, 0)$ [48] and indicated with \mathcal{D} in the picture. Normal hulls obtained via filtering \mathcal{N}_f or dicotomy \mathcal{N}_d achieve very similar results, and a Low-priority hull \mathcal{L} is provided for completeness. Finally, the figure also depicts a Critical beaconless hull \mathcal{C} , comprising 13 tuples (obtained requiring $P \geq 0.85$ for $\rho = \rho_c$ veh/km).

The same hulls are reported in Fig. 7-(b), this time considering the region above the critical density. The picture shows that the \mathcal{N}_d and \mathcal{N}_f hulls are this time a *subset* of the beaconed hull, reversing the relationship shown early in Fig. 5-(b). In other words, it is possible to make design choices such that beaconless algorithms actually outperform beaconed one with respect to both reliability and redundancy. As a side note, the dicotomic approach yields to a smaller subset of the solution space with respect to standard filtering techniques: the \mathcal{N}_d hull contains indeed only 4 algorithmic settings tuples, which are only about *one fourth* of the tuples represented by \mathcal{N}_f .

6.2. Non-ideal wireless channel

We now investigate the performance of both roadcast paradigms under lossy wireless channels. For comparison purposes, we define a beaconed reduced set \mathcal{B}'

with the same cardinality (i.e., 4 tuples) of the reduced beaconless group \mathcal{N}_d . As the adaptive margin $E_f(d, v)$ function does not yield a clear advantage, and since the beaconed hull is very compact as previously noticed, we select the four extremal points $(B, E, 0)$, where the update interval is $B \in \{1, 5\}$ s, the error margin is constant ($E_f^{ID} = 0$) and equal to $E \in \{0, 16\}$ m.

Results presented in this section refer to scenarios generated using 4 different traffic models, 2 different channel models, each tuned according to 6 different settings, running 2 classes of algorithms comprising 4 different design settings, for a total of 384 simulation points per vehicular traffic density (i.e., 6,144 settings in total). Notice that, as reported in Tab. II, loss probability ranges from 0% to 25%, so that we consider both ideal as well as lossy channels. Fig. 8-(a) depicts, for all traffic densities under both ideal and lossy channels, the number of messages versus the reception probability hull (left plot) and the delay at the end of the reception strip versus the reception probability hull (right plot). From either plot, it can be gathered that beaconless approaches are intrinsically more robust to wireless channel losses (worst case reliability of \mathcal{N}_d is twice as much that of \mathcal{B}'), due to their distributed flooding root. Another important remark is that, to the best of our knowledge, the *joint* effect of the wireless channel error and the underlying traffic model are so far unexplored, even if they can have dramatic impact on the performance: indeed, the reception probability P may drop of a factor of 2 in the beaconless case and a factor of 4 in the beaconed one.

Concerning timeliness, it can be seen that beaconless \mathcal{N}_d delay is about twice as much that of \mathcal{B}' . Yet, despite the introduction of a waiting time in the

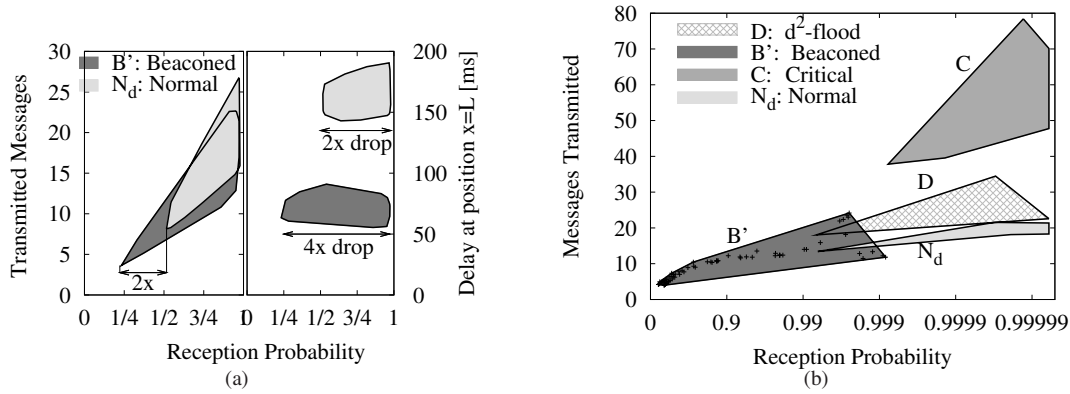


Fig. 8. Beaconned (B') and beaconless (C, D, N_d) sensitivity of the reliability, redundancy and timeliness performance to wireless channel, traffic density and traffic model variations.

beaconless approach, vehicles that are far away (i.e., 2 kilometers) at the end of the relevant strip receive the broadcast message after a delay no longer than 200 ms. Thus, during the broadcast propagation, a 100 km/hr-moving vehicle could just have moved of about 5 meters, which does not threaten the effectiveness of beaconless algorithms even for safety applications.

Performance of some of the previously considered hulls is reported again in Fig. 8-(b), this time considering both ideal as well as lossy wireless channels at jammed vehicular densities. Logarithmic scale is used for the reliability on the x-axis. It can be seen that the worst-case reliability of the Critical group C is about one order of magnitude higher with respect to N_d or D . Also, notice that both N_d and D beaconless services are in their turn much more reliable than the beaconned one B' : in this case, we plot also the individual dots within the beaconned hull, to show that most points in this case fall well below the 90% reliability threshold. Intuitively, B' is reliable over a range of traffic models and jammed densities only provided that the wireless loss rate is very low.

7. Why beaconned at all?

7.1. Reliability vs redundancy

In this section, we further stress the beaconned versus beaconless comparison, showing that the best candidate in the explored beaconless settings outperforms the best beaconned one. Focusing on

error-free wireless medium, we preliminary select the most reliable beaconned service, given by $(5, 16, 0) \in B'$ tuple, with respect to which we normalize the performance of some representative beaconless algorithms. In particular, we consider: the Critical $(3, 3, 2, 2) \in C$ tuple; the algorithm of [48], represented by $(0, 1, 8, 0) \in D$ following our notation; the Normal algorithm $(1, 4, 8, 2) \in N_d$, whose forwarding probability depends on both the distance from the originator and the vehicular speed.

Fig. 9 depicts, as a function of the vehicular traffic density, the beaconless over beaconned ratios of both (i) the number of exchanged messages in the relevant area for each roadcast message, excluding the beaconned overhead and (ii) the reception probability in the relevant area. The picture not only shows that, as expected, beaconless is largely superior to beaconned for what concerns the reception probability metric (especially around critical densities), but also shows that redundancy can be limited. More precisely, the critical group's tuple C yields to the upper bound of the reception probability, but the number of exchanged messages with respect to the beaconned case grows unbounded. The D tuple instead limits the overhead to slightly more than a factor of 2: indeed, at densities higher than $\rho > 50$ veh/km, the distance between vehicles decreases, and so does the forwarding probability $P(d) = 1 - (1 - d)^8$, which in turns decreases the number of transmitted messages.

Finally, the N_d tuple shows that when vehicles also take into account their *own speed*, they may effectively reduce the amount of transmitted messages without compromising the service reliability: indeed, notice

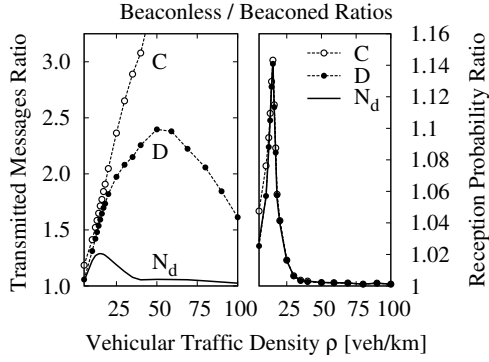


Fig. 9. Redundancy (left) and reliability (right) ratios

that in the \mathcal{N}_d case, for densities above the critical threshold $\rho > \rho_c$ the overhead decreases approaching that of the beaoned class (ratio very close to one). This is due to the fact that, in this case, vehicles reduce the rebroadcast probability not only as a function of their *distance*, but also of their *speed*. At very high densities, reduction of the forwarding probability due to decreasing inter-vehicular distance is coupled with the forwarding probability reduction due to vehicular slow-down (recall that Fig. 4-(b) shows that the average speed decreases as the vehicular density increases). In other words, vehicles can infer from their speed that they are in a high-density area or jammed, and thus avoid to rebroadcast. Moreover, redundancy increase (25% at ρ_c) is actually *needed* in order to ameliorate the reliability performance (14% at ρ_c) with respect to the beaoned baseline.

7.2. Transmission Overhead

In this section we compare the overall number of messages transmitted by the beaonless and beaoned approaches, accounting also for the messages generated by the beaoning procedure itself. Intuitively, it can be expected beaoning overhead to be excessive when either the vehicular density is high (since many vehicles participate to beaoning), or the roadcast traffic rate is low (since beaoning may constitute a non-negligible portion of the traffic).

To quantitatively perform the message overhead comparison, we derive a very simple analytical model. We assume that $S_M = 1000$ Bytes long new roadcast messages are generated at a rate λ_M . In order to compute the number of transmitted messages per

each broadcast packet, we select the $(1, 4, 8, 2) \in \mathcal{N}_d$ beaonless strategy, and denote by $\text{Beaonless}(\rho)$ the number of relay messages per roadcast message over the road L , obtained by simulation for a density ρ . Similarly, we denote by $\text{Beaoned}(\rho)$ the number of relay messages in the beaoned algorithm $(5, 16, 0) \in \mathcal{B}'$. In the beaoned case, we explicitly account for beacons, assuming that beaoning procedure sends S_B long beacons at a rate $\lambda_B = 1/B = 0.2$ Hz. We evaluate the beaonless over beaoned message overhead ratio $O_M(\rho, \lambda_M)$ as a function of the density ρ and roadcast rate λ_M as:

$$O_M = \frac{\lambda_M S_M \text{Beaonless}(\rho)}{\lambda_M S_M \text{Beaoned}(\rho) + \lambda_B S_B \rho L} \quad (1)$$

Results for (1) are reported in Fig. 10. Specifically, Fig. 10-(a) depicts the $O_M(\rho, \lambda_M)$ surface on the z-axis, as a function of the vehicular traffic density ρ on the x-axis and of the broadcast traffic rate λ_M on the y-axis. Fig. 10-(a) also reports, on the xy plane, the contour lines of (1), i.e., the equipotential curves defined as the locus of points $\{(\rho, \lambda_M) : O_M(\rho, \lambda_M) = O_i\}$, where O_i is a constant (and in the case of figure O_i has been chosen in the set $\{0.25, 0.5, 0.75, 1, 1.1, 1.2, 1.3\}$ for the different contour lines). Intuitively, contour lines for the $O_M(\rho, \lambda_M)$ surface can be obtained by projecting on the xy plane, the intersection of the $O_M(\rho, \lambda_M)$ surface with planes sited at different heights on the z-axis and parallel to the xy plane. Let us now focus on the contour plots representation of the beaonless/beaoned overhead ratio $O_M(\rho, \lambda_M)$, which is reported in Fig. 10-(b) for $S_B = 500$ Bytes (left) and $S_B = 20$ Bytes (right). Gray shaded zones indicate areas where the beaoning overhead is so intense that the beaoned approach is more resource consuming than beaonless one (i.e., $O_M(\rho, \lambda_M) < 1$). In other words, gray zones correspond to network operation points where beaoning overhead overwhelms beaonless redundancy. If we consider that for security reasons, vehicles may need to add a key to authenticate the beaon message (and they may need to add both vehicle manufacturer as well as state regulator keys in the same message), the beaon size will likely increase. Clearly, considering $S_B = 500$ as in the left portion of the picture, the comparison is even more favorable to beaonless paradigm.

The most interesting result is that in no case the beaonless overhead exceeds 30%: as stated before, around the critical density the redundancy is actually *needed* to ameliorate the broadcast reliability.

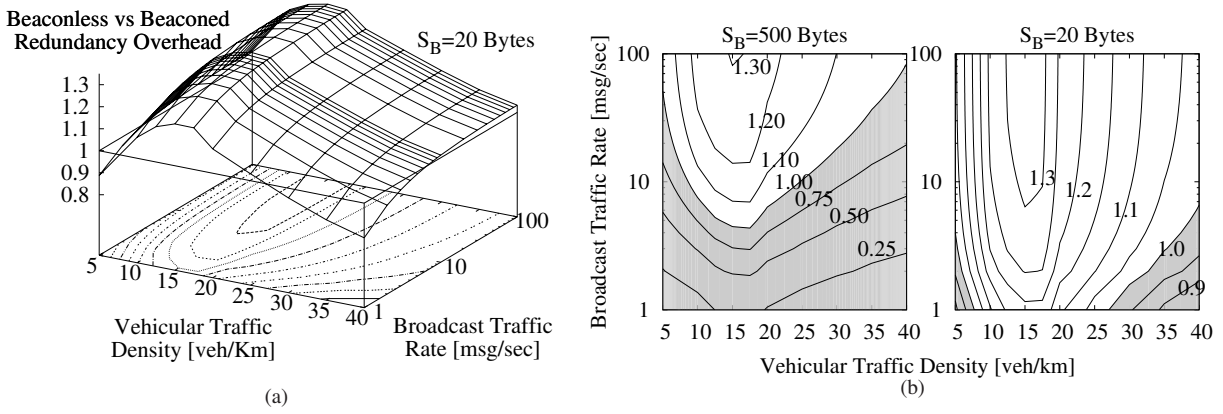


Fig. 10. Beaconless/beaconed redundancy ratio $O_M(\rho, \lambda_M)$: (a) three-dimensional surface and (b) contour plots for beacon sizes of 500 Bytes (left) and 20 Bytes (right).

7.3. Channel Occupancy

Finally, we evaluate the bandwidth occupancy of the beaconless versus beaoned paradigm roadcast, or, in other words, we evaluate how much bandwidth is left to other transmissions on the same channel. Notice that such bandwidth may be used e.g., for broadcast as well as for unicast services. Considering a 802.11 MAC layer, we denote with $T_{bck} = 67.5 \mu\text{s}$ the average backoff time, and with $DIFS = 34 \mu\text{s}$ the inter-frame space sequence. We recall that C is the link data-rate, and that S_M and S_B indicate the message and beacon size, respectively.

We have that, in the beaconless case, the transmission of each message has a duration equal to $T_{tx}(S_M) = T_{bck} + DIFS + 8S_M/C$, independently of the used algorithm. We then evaluate the number of roadcast transmissions in the collision range of a node, which is given by the number of relay nodes of the beaconless algorithm in the $2R$ long road stretch centered around the node. Recalling that we denoted by $\text{Beaconless}(\rho)$ the empirical number of messages in the relevant area L , gathered by simulation, we have that the number of roadcast transmissions in the collision range is $\text{Beaconless}(\rho) \frac{2R}{L}$. Thus, each node senses the medium busy for a time $T_{busy}(\rho, S_M) = \text{Beaconless}(\rho) \frac{2R}{L} T_{tx}(S_M)$, since no ACK follows the roadcast transmission.

Similarly, a roadcast transmission in the beaoned case occupies the medium for a time $T'_{busy}(\rho, S_M) = \text{Beaoned}(\rho) \frac{2R}{L} T_{tx}(S_M)$, to which the medium occupancy due to the beacons transmission has to be added. Beacons transmission time is given

by the duration of a single beacon transmission, $T_{tx}(S_B) = T_{bck} + DIFS + 8S_B/C$, multiplied by the number of vehicles in the transmission range, thus $T'_{beacon}(\rho, S_B) = \rho 2R T_{tx}(S_B)$.

Denoting with λ_M the broadcast messages traffic rate, and with $\lambda_B = 1/B$ the beacon rate, we can then evaluate the ratio of the beaconless versus beaoned channel occupancy $O_C(\rho, S_M, S_B, \lambda_M, \lambda_B)$ as:

$$O_C = \frac{\lambda_M T_{busy}(\rho, S_M)}{\lambda_M T'_{busy}(\rho, S_M) + \lambda_B T'_{beacon}(\rho, S_B)} \quad (2)$$

We depict (2) in Fig. 11 for different combinations of the system parameters. We again focus on error-free wireless medium and consider the beaoned $(5, 16, 0) \in \mathcal{B}'$ and beaconless $(1, 4, 8, 2) \in \mathcal{N}_d$ settings. In order to gather conservative results, we focus on critical vehicular density ρ_c which yield (as shown early in Fig. 9 and Fig. 10) to an upper bound of the channel occupancy in the beaconless case. Left-hand side of Fig. 11 depicts the channel occupancy ratio O_C as a function of the λ_M/λ_B ratio for different message and beacon size pairs (S_M, S_B) . First, notice that channel occupancy ratio is never larger than 1.3, irrespectively of the λ_M/λ_B ratio. When beacons are 500 Bytes long, the beaoned procedure is profitable provided that the traffic rate exceeds the beacon rate by at least a factor 3 (when messages are 1000 Bytes long), or by a factor 10 (when beacons and messages sizes are comparable). This means that, for a beaoning interval of $B = 5$ s, between 15–50 new messages per second have to be generated to offset the baseline beaoning cost. Clearly, the

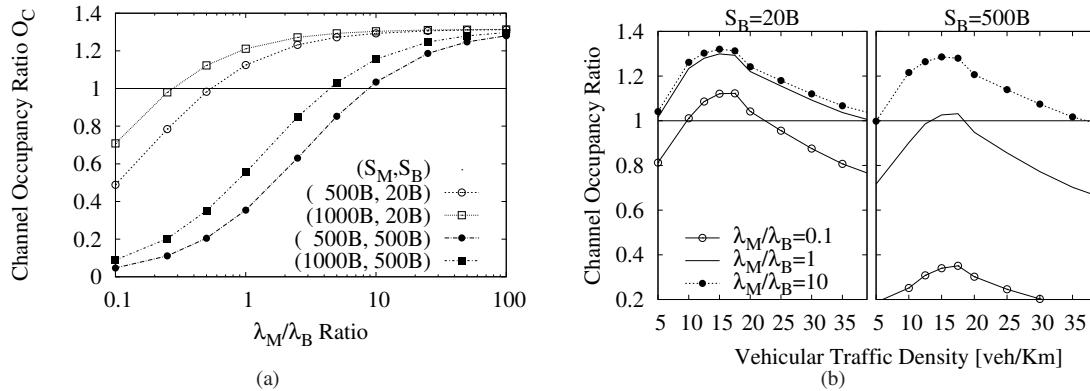


Fig. 11. Beaconless/beaconed channel occupancy ratio $O_C(\cdot)$ as a function of (a) λ_M/λ_B and of (b) the vehicular density ρ

number of messages is high considering safety or road-informations systems only, but may become acceptable depending on the success of commercial roadcast advertisement services.

Right-hand side of Fig. 11 depicts instead the channel occupancy ratio as a function of the vehicular traffic density, for different levels of roadcast service usage – ranging from intensive ($\lambda_M/\lambda_B = 10$) to sporadic ($\lambda_M/\lambda_B = 1/10$) message generation rates for a fixed $B = 5$ s beaconing interval. We consider both small and large beacons, while we fix message size to $S_M = 1000$ Bytes. Curves once more confirm that beaconed service allows a gain in terms of channel utilization only provided that there is a sustained service usage, and that message size is large with respect to beacon size. As expected, such gain is more pronounced around the critical traffic density, where however reliability has been traded for redundancy in the beaconed case.

8. Conclusion

Multi-hop ad hoc broadcast services may be implemented using either *beaconed* or *beaconless* strategies: by means of simulation, we explored a fairly large algorithmic *design* space, taking into account the most important information that can be used to build efficient broadcast algorithms. Using a realistic microscopic model to represent vehicular traffic, we investigated the performance of the above classes on a broad *environmental* parameter set.

Our main contributions are the following. First, results were gathered and presented through the use

of a Convex Hull framework: the framework is very powerful in that it allows to compactly compare any performance metric of interest, and explore a wealth of design and environmental parameters. In a sense, we may say that the convex hull representation is less “misleading” than a single curve, since it individuates different “regions” in which realistic performance may fall – rather than aiming at precisely quantifying real-world performance by means of simulation, which forcibly reflects a number of simplifying assumptions.

Second, we showed that in the beaconless case, taking into account vehicular speed can very effectively assist the rebroadcast decision – both to increase the reception probability at low vehicular densities (and thus, high speeds) and to decrease the overhead at high densities (and thus, low speeds).

Third, the above findings lead to the conclusion that the beaconing approach is not justified for near-field single-shot information dissemination in suburban and highway VANETs. More precisely, in jammed or near jammed highway scenarios, beaconless dissemination is more reliable (i.e., higher reception probability) and more efficient (i.e., lower number of messages), provided that the overhead of the beaconing procedure is taken into account. Moreover, in lower-density VANETs, the additional amount of messages exchanged by beaconless algorithms is actually *needed* in order to ameliorate the reliability of the roadcast service in critical situations. Thus, there is no evident performance gain to justify the complexity entailed by the beaconing procedure in the considered scenarios.

References

1. D. Rossi, R. Fracchia and M. Meo, "VANETs: Why Beaconing at All?". *Proc. of IEEE International Conference on Communications (ICC'08)*, Beijing, China, May 2008.
2. J. Blum, A. Eskandarian, L.J. Hoffman, "Challenges of Intervehicle Ad Hoc Networks," *IEEE Transactions on Intelligent transportation Systems*, Vol.5, No.4, Dec. 2004, pp.347-351.
3. A. K. Saha and D. Johnson. "Modeling mobility for vehicular ad hoc networks" *Proc. of ACM VANET'04*, Philadelphia, PA, USA, Oct. 2004.
4. D. R. Choffnes and F. E. Bustamante, "An integrated mobility and traffic model for vehicular wireless networks," *Proc. of ACM VANET'05*, Cologne, Germany, Sep. 2005.
5. M. Kim, D. Kotz, and S. Kim, "Extracting a mobility model from real user traces," *Proc. of IEEE INFOCOM'06*, Barcelona, Spain, Apr. 2006.
6. M. M. Artimy, W. Robertson, W. J. Phillips, "Connectivity in Inter-Vehicle Ad Hoc Networks," *Proc. of 17th IEEE Canadian Conference on Electrical and Computer Engineering (CCECE'04)*, Niagara Falls, Canada, May 2004.
7. R. Fracchia, M. Meo and D. Rossi, "On the Impact of Traffic Models on Inter-vehicular Broadcast Communication" *Proc. of MedHocNet'06*, Lipari, Italy, Jun. 2006
8. X. Zhang, J.K. Kurose, B.N. Levine, D. Towsley, H. Zhang, "Study of a bus-based disruption tolerant network: Mobility modeling and impact on routing," *In Proc. of ACM MOBICOM'07*, Montreal, Canada, Sep. 2007.
9. M. Fiore, J. Härrä "The Networking Shape of Vehicular Mobility", *Proc. of ACM MOBIHOC'2008*, Hong Kong, CN, May 2008.
10. Torrent-Moreno, M., Jiang, D., Hartenstein, H., 2004. "Broadcast Reception Rates and Effects of Priority Access in 802.11-based Vehicular Ad-hoc Networks," *Proc. of ACM VANET'04*, Philadelphia, PA, USA, Oct. 2004.
11. H. F. Wedde, S. Lehnhoff, B. van Bonn "Highly Dynamic and Scalable VANET Routing for Avoiding Traffic Congestions," *Proc. of ACM VANET'07*, Montreal, Quebec, 2007
12. Y.B. Ko, N.H. Vaidya, "Location-Aided Routing (LAR) in Mobile Ad Hoc Networks," *Proc. of ACM MOBICOM'98*, Dallas, TX, USA, Oct. 1998.
13. G.Korkmaz, E. Ekici, G. Özgüner, Ü Özgüner, "Urban Multi-Hop Broadcast Protocol for Inter-Vehicle Communication Systems," *Proc. of ACM VANET'04*, Philadelphia, PA, USA, Oct. 2004.
14. J. Zhao, G. Cao, "VADD: Vehicle-Assisted Data Delivery in Vehicular Ad Hoc Networks" *IEEE Transactions on Vehicular Technology*, Vol. 57, No.3, May 2008
15. H. Wu, M Palekar, R Fujimoto, R Guensler, M Hunter, J. Lee and J. Ko "An empirical study of short range communications for vehicles," *Proc. of ACM VANET*, Cologne, Germany, 2005
16. A. Behzad, I. Rubin, "Impact of Power Control on the Performance of Ad Hoc Wireless Networks," *Proc. of IEEE INFOCOM'05*, Miami, FL, Mar. 2005
17. M. Torrent-Moreno, P. Santi, H. Hartenstein, "Fair Sharing of Bandwidth in VANETs," *Proc. of ACM VANET'05*, Cologne, Germany, Sep. 2005
18. Q. Chen, D. Jiang, V. Taliwal, L. Delgrossi, "IEEE 802.11 based vehicular communication simulation design for NS-2," *Proc. of ACM VANET'06*, Los Angeles, CA, USA, Sep. 2006.
19. M. Torrent-Moreno, D. Jiang, H. Hartenstein, "Broadcast Reception Rates and Effects of Priority Access in 802.11-Based Vehicular Ad-Hoc Networks," *Proc. of ACM VANET'04*, Philadelphia, USA, Oct. 2004
20. X. Yang, J. Liu, F. Zhao, N. H. Vaidya, "A Vehicle-to-Vehicle Communication Protocol for Cooperative Collision Warning," *Proc. of MobiQuitous'04*, Boston, MA, USA, Aug. 2004
21. Q. Xu, T. Mak, J. Ko, R. Sengupta, "Vehicle-to-Vehicle Safety Messaging in DSRC," *Proc. of ACM VANET'04*, Philadelphia,

- PA, USA, Oct. 2004
22. H. Alshaer, E. Horlait, "An optimized adaptive broadcast scheme for inter-vehicle communication," *IEEE Vehicular Technology Conference (VTC'05)*, Stockholm, Sweden, May 2005
 23. T. ElBatt, S. K. Goel, G. Holland, H. Krishnan, J. Parikh, "Cooperative collision warning using dedicated short range wireless communications," *Proc. of ACM VANET'06*, Los Angeles, USA, Sep. 2006
 24. C. L. Robinson, L. Caminiti, D. Caveney, K. Laberteaux "Efficient coordination and transmission of data for cooperative vehicular safety applications," *Proc. of ACM VANET'06*, Los Angeles, CA, USA, Sep. 2006
 25. F. Yu, S. Biswas, "Self-Configuring TDMA Protocols for Enhancing Vehicle Safety With DSRC Based Vehicle-to-Vehicle Communications," *IEEE Journal on Selected Areas in Communications*, Vol. 25, No. 8, Oct. 2007
 26. IEEE Std 802.11p, Wireless Access in Vehicular Environments (WAVE)
 27. H. Menouar, F. Filali, M. Lenardi, "A survey and qualitative analysis of MAC protocols for vehicular ad hoc networks," *IEEE Wireless Communications*, Vol.13, No.5, pp.30-35, Oct. 2006
 28. James Bernsen and D. Manivannan, "Unicast Routing Protocols for Vehicular Ad Hoc Networks: A Critical Comparison and Classification", *Pervasive and Mobile Computing, Elsevier*, Vol. 5, 2009
 29. V. Naumov, R. Baumann, and T. Gross, "An evaluation of inter-vehicle ad hoc networks based on realistic vehicular traces" *Proc. of ACM MOBIHOC'06*, Florence, Italy, May 2006
 30. N. Wisitpongphan, F. Bai, P. Mudalige, V. Sadekar and O. Tonguz, "Routing in Sparse Vehicular Ad Hoc Wireless Networks", *IEEE Journal on Selected Areas in Communications*, Vol. 25, No. 8, Oct. 2007
 31. M. Garcia De La Fuente and H. Labiod, "A performance comparison of position-based routing approaches for mobile ad hoc networks," *Proc. of IEEE Vehicular Technology Conference (VTC'07)*, Baltimore, MD, USA, Sep. 2007.
 32. F. Borgonovo, A. Capone, M. Cesana, L. Fratta, "ADHOC MAC: A New MAC Architecture for Ad Hoc Networks Providing Efficient and Reliable Point-to-Point and Broadcast Services," *Wireless Networks*, Vol. 10, Jul. 2004.
 33. C. E. Perkins, E. Royer, and S. Das, "Ad hoc on demand distance vector (AODV) routing," *IETF RFC 3561*, Jul. 2003.
 34. B. Karp, H.T. Kung, "GPSR: Greedy Perimeter Stateless Routing for Wireless Networks," *Proc. of ACM MOBIHOC'00*, Boston, MA, USA, Aug. 2000.
 35. D. B. Johnson, D. Maltz, and Y. Hu, "Dynamic source routing protocol for mobile ad hoc networks (DSR)", *IETF Internet Draft*, Apr. 2003
 36. S. Basagni, I. Chlamtac, V.R. Syrotiuk, B.A. Woodward, "A distance routing effect algorithm for mobility (DREAM)," *Proc. of ACM MOBIHOC'98*, Dallas, TX, USA, Oct. 1998.
 37. A. Capone, L. Pizziniaco, I. Filippini, M.A.G de la Fuente, "A SiFT: an efficient method for trajectory based forwarding," *In 2nd International Symposium on Wireless Communication Systems*, Sep. 2005
 38. B. Williams, T. Camp, "Comparison of Broadcast Techniques for Mobile Ad Hoc Networks," *Proc. of ACM MOBIHOC'02*, Lausanne, Switzerland, Jun. 2002
 39. Y.C. Tseng, S.Y. Ni, E.Y. Shih, "Adaptive approaches to relieving broadcast storms in a wireless mulihop mobile ad hoc network," *IEEE Transactions on Computers*, Vol. 52, No. 5, May 2003, pp.545-557.
 40. M. Mauve, A. Widmer, H. Hartenstein, "A survey on position-based routing in mobile ad hoc networks," *IEEE Network Magazine*, Vol. 15, No. 6, Nov. 2001, pp. 30-39.
 41. R. Fracchia, M. Meo, and D. Rossi, "Knowing Vehicle Location HELPs Avoiding Broadcast Packets Storm," *Proc. of*

- MP2P Workshop at IEEE PerComm'06*, Pisa, Italy, March 17, Mar. 2006.
42. S.Y. Ni, Y.C. Tseng, Y.S. Chen, J.P. Sheu, "The broadcast storm problem in a mobile ad hoc network," *Proc. of ACM MOBICOM'99*, Seattle, WA, US, Aug. 1999.
 43. L.B. Briesemeister, L. Shafers, G. Hommel, "Disseminating Messages among Highly Mobile Hosts based on Inter-Vehicle Communications," *IEEE Intelligent Vehicles Symposium*, Oct. 2000.
 44. M. Heissenbüttel, T. Braun, T. Bernoulli, M. Wälchli "BLR: beacon-less routing algorithm for mobile ad hoc networks," *Elsevier Computer Communications*, Vol. 27, No. 11, Jul. 2004.
 45. Füßler, M. Mauve, H. Hartenstein, D. Vollmer and M. Käsemann, "Location based routing for vehicular ad-hoc network," *Proc. of ACM MOBICOM'02*, Atlanta, GA, USA, Sep. 2002
 46. H. Füßler, J. Widmer, M. Käsemann, M. Mauve, H. Hartenstein "Contention-Based Forwarding for Mobile Ad-Hoc Networks" *Elsevier's Ad Hoc Networks*, Vol. 1, No. 4, Nov. 2003
 47. C. Lochert, M. Mauve, H. Füßler, H. Hartenstein "Geographic Routing in City Scenarios," *ACM Mobile Computing and Communications Review*, Vol. 9, No. 1, Jan. 2005
 48. R. Fracchia, M. Meo, and D. Rossi, "Avoiding broadcast storms in inter-vehicular warning delivery services," *Proc. of Application and Services in Wireless Networks (ASWN'06)*, Berlin, Apr. 2006
 49. I. Leontiadis, C. Mascolo, "Opportunistic spatio-temporal dissemination system for vehicular networks" *1st ACM Workshop on Mobile Opportunistic Networking (MobiOpp'07)*, Puerto Rico, Jun. 2007
 50. R. Fracchia, M. Meo: "Analysis and Design of Warning Delivery Service in Intervehicular Networks," *IEEE Transactions on Mobile Computing*, Vol. 7 No. 7, 2008.
 51. Wireless on Wheel Simulator (wowSim), available at <http://www.enst.fr/~drossi/wowSim>
 52. G. Anastasi, E. Borgia, M. Conti, E. Gregori and A. Passarella, "Understanding the real behavior of Mote and 802.11 ad hoc networks: an experimental approach," *Pervasive and Mobile Computing (Elsevier)*, Vol. 1, Jul. 2005, pp. 237-256
 53. M. Zuniga and B. Krishnamachari, "Analyzing the Transitional Region in Low Power Wireless Links," *Proc. of IEEE SECON'04*, Santa Clara, CA, USA, Oct. 2004
 54. E.N. Gilbert, "Capacity of a burst-noise channel," *Bell Syst. Tech. J.*, p. 1253, Sep. 1960
 55. V. Taliwal, D. Jiang, H. Mangold, C. Chen, R. Sengupta, "Empirical determination of channel characteristics for DSRC vehicle-to-vehicle communication", *Proc. of ACM VANET'04*, Philadelphia, PA, USA, 2004
 56. K. Nagel and M. Schreckenberg, "A cellular automaton model for freeway traffic," *J. Phys. I2*, pp.2221-2229, 1992.
 57. R. Barlovic, L. Santen, A. Schadschneider and M. Schreckenberg, "Metastable states in CA models for traffic flow," *Eur. Phys. J. B.*, (5)1998, pp. 793-800.
 58. W. Brilon and N. Wu, "Evaluation of Cellular automaton for Traffic Flow Simulation on Freeway and Urban Streets", *In Traffic and Mobility, Springer Verlag (Berlin)*, 1999.
 59. P.G. Gipps, "A behavioural car following model for computer simulation," *Transportation Res. B*, (15)1981, pp. 105-111.
 60. F.L. Hall, B. Allen and M.A. Grunter, "Empirical analysis of freeway flow-density relationships," *Tran. Res. A* 20, pp. 191-201, 1987.
 61. B.S. Kerner, "Experimental features of the emergence of moving jams in free traffic flow," *J. Phys. A* 33, pp. 221-228, 2000.
 62. C.E. Palazzi, S. Ferretti, M. Rocchetti, G. Pau, M. Gerla, "How Do You Quickly Choreograph Inter-Vehicular Communications? A Fast Vehicle-to-Vehicle Multi-Hop Broadcast Algorithm, Explained," *Proc IEEE CCNC'2007*, Jan. 2007